

Mav_9

9 DOF Humanoid Robotic ARM

Development Document

Team Mavericks

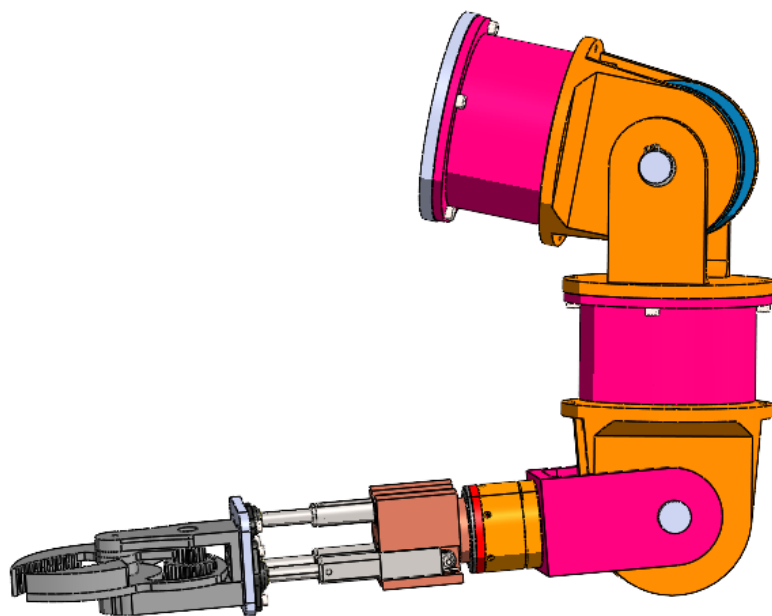
A Akash (MS/EAV4-PS)

Ansel Sebastian (MS/EAV4/PS)

Arun Mathew (MS/EAII2-PS)

Bosch FIT.Fest '25

November 30, 2025



Contents

1 Project Overview and Objective	8
1.1 Product Concept	8
1.2 Project Repository	8
1.3 Tools and Resources	8
1.4 The 9-DOF Architecture	9
2 System Architecture and Innovation	11
3 Mechanical Design and Packaging	12
3.1 Sub System 1: Shoulder System	12
3.2 Sub System 2: Elbow System	13
3.3 Sub System 3: Forearm & Gripper	13
4 Motion Validation and Kinematics	14
4.1 Initial Hand Calculations	14
4.1.1 4.1.1 Torque Calculation & Static Validation	14
4.2 Kinematic Diagram & Analysis	15
4.2.1 Subsystem 1: Shoulder Complex (Spherical Topology)	15
4.2.2 Subsystem 2: Elbow & Forearm (2-DOF Serial)	16
4.2.3 Subsystem 3: Parallel Wrist & Gripper (3-DOF Parallel)	17
4.3 Full System Kinematic Modeling	21
4.3.1 Global Kinematic Diagram	22
4.3.2 Global Denavit-Hartenberg (DH) Parameters	22
5 Digital Twin & Simulation Framework	23
5.1 Simulation Architecture Overview	23

5.2	Kinematic Modeling Implementation	23
5.2.1	DH Integration	23
5.2.2	Forward Kinematics (FK) Pipeline	24
5.3	Inverse Kinematics (IK) Strategy	24
5.4	Interactive GUI & User Experience	24
5.5	System Validation & Safety Features	26
6	Static Structural Analysis	26
6.1	Component Analysis: Shoulder/Elbow Bracket	27
6.1.1	Setup and Boundary Conditions	27
6.1.2	Results and Safety Factor	27
6.2	System Analysis: Full Robot Assembly	28
6.2.1	Simulation Setup	28
6.2.2	Deformation and Stress Results	29
6.3	Modal Analysis (Frequency Response)	31
6.3.1	Results: Eigenmode Visualization	31
6.3.2	Resonance Risk Assessment	33
6.3.3	Actuator Operating Frequency Spectrum	33
6.3.4	Conclusion: Critical Resonance Assessment	34
7	Costing and Supply Chain Strategy	35
7.1	Component Selection	35
8	DFMEA	36
9	Future Road Map (Version 2.0)	40
9.1	V1.5: Production Readiness	40
9.2	V2.0: The "Smart" Arm	40

9.3	V3.0: Ecosystem Expansion	40
-----	---------------------------	----

10	Conclusion	41
-----------	-------------------	-----------

List of Figures

1	Requirement from RFP	8
2	Mavericks Design	8
3	Shoulder Assembly	10
4	Shoulder Assembly	10
5	Forearm Assembly	11
6	Stewart Platform (Courtesy: Arduino, 3D model by barracuda)	12
7	Shoulder Subsystem	13
8	Shoulder Actuators	13
9	Forearm CAD Assembly: Housing Linear Drives and Gripper Interface	14
10	Static Load Diagram: Rotary Shoulder & Elbow	15
11	Kinematic Diagram: Shoulder Complex (Exploded View of Intersecting Axes) .	16
12	Kinematic Diagram: Elbow & Forearm	16
13	Kinematic Diagram: 3-UPS Parallel Wrist	17
14	Platform Geometry - Front View	19
15	Yaw Motion Top View	19
16	Pitch Motion Side View	20
17	Global Kinematic Diagram (8-DOF Chain)	22
18	GUI Interface: Target Inputs, Live Joint Telemetry, and Solver Status	25
19	Real-Time 3D Visualization of the Maverick-9 Kinematic Chain	25
20	Safety Logic: System rejecting an out-of-bounds target command	26
21	Bracket Mesh Density	27
22	Von Mises Stress Distribution	27
23	Stress Concentration Zoom at Fastener Interface	28
24	Full Assembly Simulation Setup (Gravity + 8kg Payload)	29

25	Full Assembly Mesh Generation	29
26	Displacement Magnitude Plot (Cantilever Effect)	30
27	Global Von Mises Stress Distribution	30
28	Mode 1: 60.96 Hz	32
29	Mode 2: 65.4 Hz	32
30	Mode 3: 195.6 Hz	32
31	Mode 4: 222.0 Hz	32
32	Mode 5: 454.0 Hz	32
33	Mode 6: 485.6 Hz	32
34	First 6 Eigenmodes showing structural deformation patterns.	32
35	Mode 7: 541.0 Hz	33
36	Mode 8: 618.5 Hz	33
37	Mode 9: 713.9 Hz	33
38	Mode 10: 838.2 Hz	33
39	Higher-order Eigenmodes (Modes 7-10).	33

List of Tables

1	DH Parameters: Spherical Shoulder	16
2	DH Table for Subsystem 2 (Elbow & Forearm)	17
3	Parallel Actuation Logic	18
4	Equivalent Virtual DH Table for Tripod Wrist	18
5	Complete 8-DOF System DH Table with Joint Limits	22
6	System Excitation Spectrum at Rated Load	34
8	DFMEA for Hybrid Kinematic Design	37

1 Project Overview and Objective

1.1 Product Concept

The **Maverick-9** is a next-generation humanoid robotic manipulator designed to meet the rigorous demands of the Bosch FIT.Fest '25 challenge. Our objective was to engineer a robotic limb capable of lifting a 5kg payload with full human-like dexterity, while adhering to strict mass-production standards. Unlike traditional serial manipulators that suffer from compounding weight at the extremities, the Maverick-9 utilizes a bio-mimetic, distributed actuation strategy.

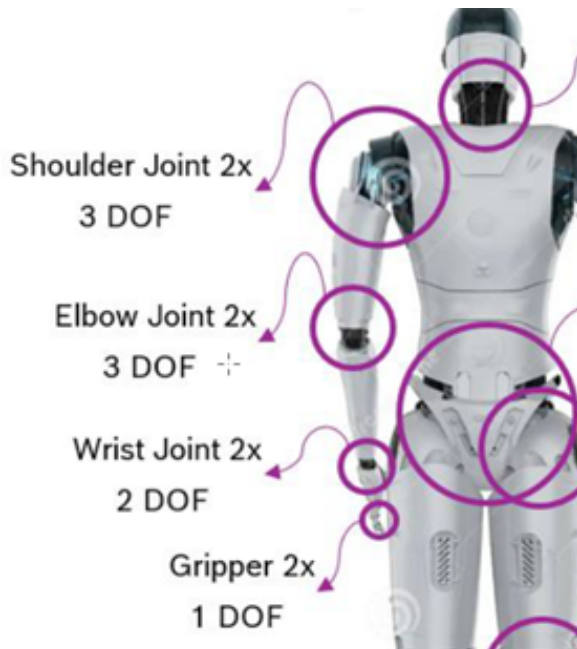


Figure 1: Requirement from RFP

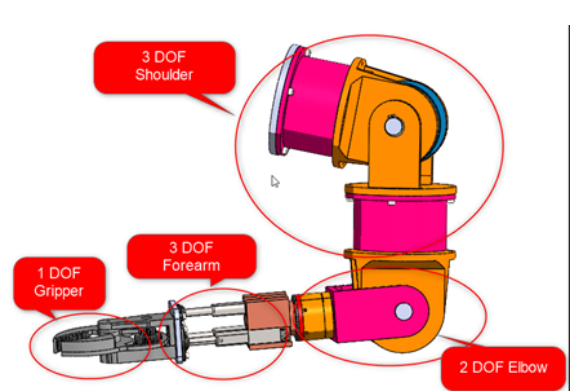


Figure 2: Mavericks Design

1.2 Project Repository

The complete source code, CAD models, and simulation framework are available for review in our open-source repository:

- GitHub: [devArun-13/MAV_9](#)
This is the 9 DOF System Made for Bosch Fit Fest 2025.

1.3 Tools and Resources

The development and documentation of the Maverick-9 robotic arm utilized a suite of cloud-based and computational tools to ensure design accuracy and collaboration.

- **Onshape:** Cloud-native CAD platform used for the parametric 3D modeling of the entire assembly, interference checking, and generating manufacturing drawings.
- **SimScale:** Cloud-based simulation platform utilized for Finite Element Analysis (FEA) to validate the structural integrity and safety factors of the die-cast aluminum joints.
- **Python:** Programming language used to calculate Denavit-Hartenberg (DH) parameters, validate inverse kinematics algorithms, and generate torque curve plots.
- **Google Scholar:** Research database leveraged to source academic papers on parallel mechanisms, kinematic topologies, and OEM component datasheets.
- **Overleaf:** Collaborative online L^AT_EX editor used for the typesetting, formatting, and version control of this technical documentation.
- **Google Gemini:** AI assistant utilized as a thought partner for code debugging, text summarization, and L^AT_EX syntax optimization.
- **Claude:** AI assistant leveraged for the architectural development of the "Maverick-9 Studio" Digital Twin, specifically for implementing the numerical inverse kinematics solver and the real-time Python GUI framework.

1.4 The 9-DOF Architecture

To achieve the required 9 Degrees of Freedom (DOF) while maintaining structural rigidity and optimizing the center of mass, we have architected the system into three distinct, modular subsystems:

Subsystem 1: The Shoulder Power Core (3 DOF)

Designed as the high-torque anchor of the system, this module utilizes three **CubeMars AK80-64** actuators to provide the heavy lifting capabilities (Roll, Pitch, Yaw) required to support the entire arm lever arm at full extension.

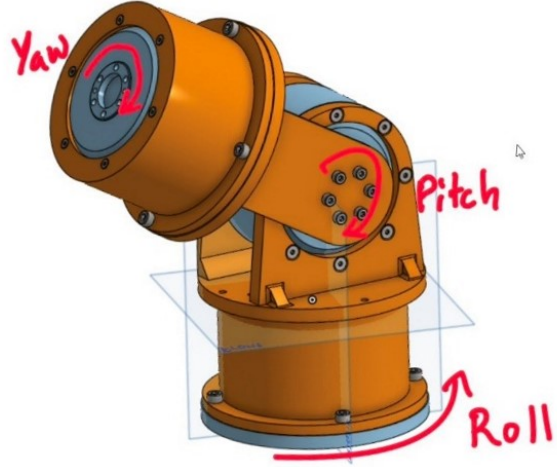


Figure 3: Shoulder Assembly

Subsystem 2: The Bicep & Elbow Rotary Drive (1 DOF)

Focusing on the "Heavy Lift" capability. It utilizes a Simple Revolute joint to execute the Elbow Flexion (Curl), maximizing mechanical advantage to lift the 5kg payload with minimal motor strain.

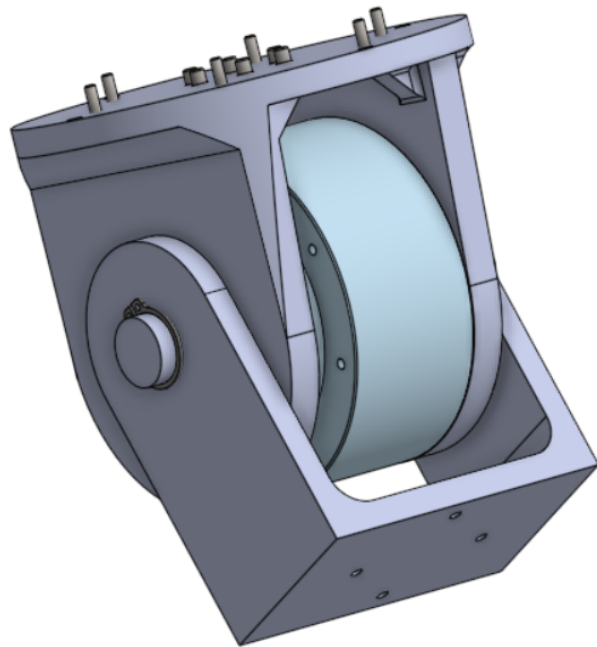


Figure 4: Shoulder Assembly

Subsystem 3: The Dexterous Forearm Complex (5 DOF)

This multi-functional module handles the fine manipulation. It integrates:

- **Forearm Roll (1 DOF):** A dedicated servo (RMD-X4) for supination/pronation.

- **Parallel Wrist (3 DOF):** A lightweight 3-UPS Linear Tripod mechanism that provides Pitch, Yaw and extend.
- **Gripper (1 DOF):** An integrated end-effector for object interaction.

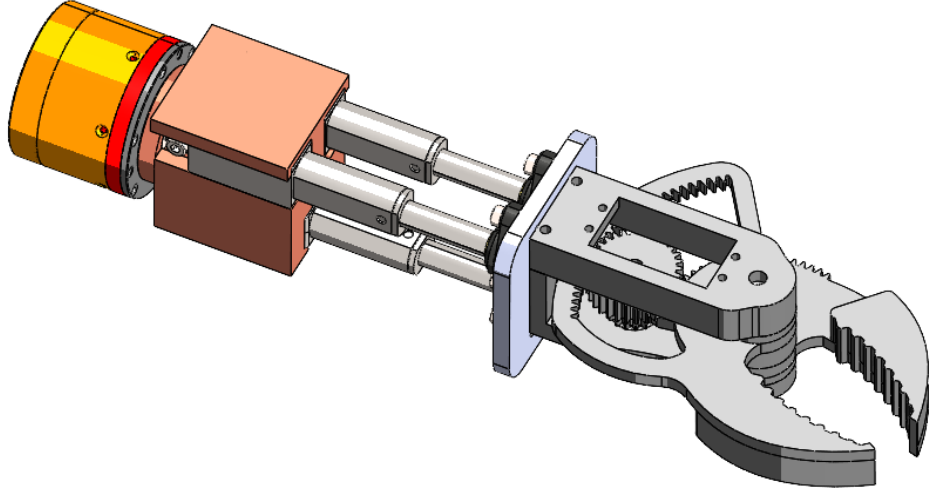


Figure 5: Forearm Assembly

This tripartite structure allows for independent assembly, simplified maintenance, and a significant reduction in distal inertia, ensuring the arm is not just powerful, but also responsive and safe for human collaboration.

TOTAL NO OF DOF = 9

2 System Architecture and Innovation

To solve the critical challenge of "Distal Mass" (weight at the end of the arm), we adopted a **Proximal Actuation Strategy** and a hybrid serial-parallel architecture.

- **1. The "Power Core" Shoulder (3-DOF Serial):**
 - **Strategy:** We prioritize pure holding power and reliability at the base.
 - **Actuation:** 3x CubeMars AK80-64 KV80 actuators.
 - **Validation:** With a rated torque of 48 Nm (Peak 120 Nm), these motors provide a Safety Factor of > 2.0x for the 5kg payload at full extension (0.6m), eliminating the risk of thermal saturation during static holding tasks.

- 2. The "Distributed" Elbow Complex (1+1 DOF):
 - **Strategy:** To satisfy the complex "3-Axis Elbow" requirement without structural weakness, we decoupled the motions.
 - **Flexion (Curl):** Achieved via a Linear Bell-Crank Mechanism. This provides massive mechanical advantage for lifting the forearm, far superior to a direct-drive motor.
 - **Supination (Roll):** Achieved via a dedicated MyActuator RMD-X4 module located in the forearm. This separates the "Twist" from the "Lift," mimicking the human radius/ulna bone structure and preventing gimbal lock.
- 3. The "Agile Eye" Wrist (3-DOF Parallel Tripod):
 - **Innovation:** Instead of a heavy serial wrist, we utilize a 3-UPS Parallel Mechanism (Tripod).
 - **Benefit:** This allows for simultaneous Pitch, Yaw, and micro-Roll adjustments.
 - **Mass Reduction:** By moving the 3 linear actuators back into the forearm, we reduce wrist inertia by $\sim 60\%$, allowing for faster, safer movements.
 - **Inspiration:** Inspired from Stewart Platform.

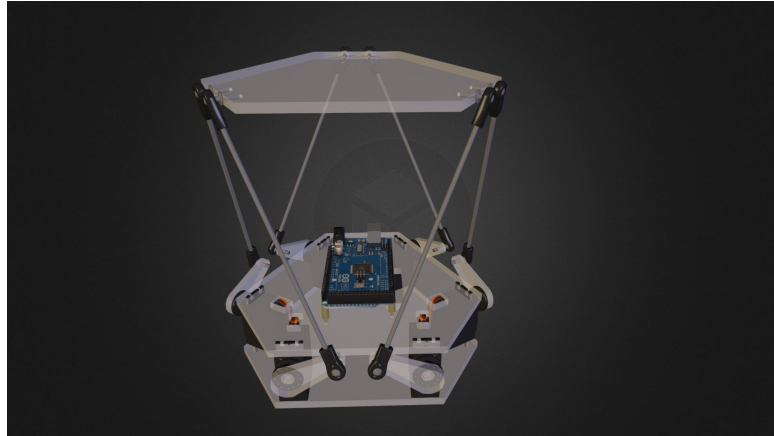


Figure 6: Stewart Platform (Courtesy: Arduino, 3D model by barracuda)

3 Mechanical Design and Packaging

3.1 Sub System 1: Shoulder System

The Shoulder Power Core is the high-torque anchor of the system.

- **Actuators:** 3x CubeMars AK80-80 (High Torque Density).

- **Function:** Provides Roll, Pitch, and Yaw for the entire arm lever.
- **Packaging:** Utilizes a dual-supported yoke design to support the motor shaft on both sides, eliminating cantilever bearing failure under the 5kg load.

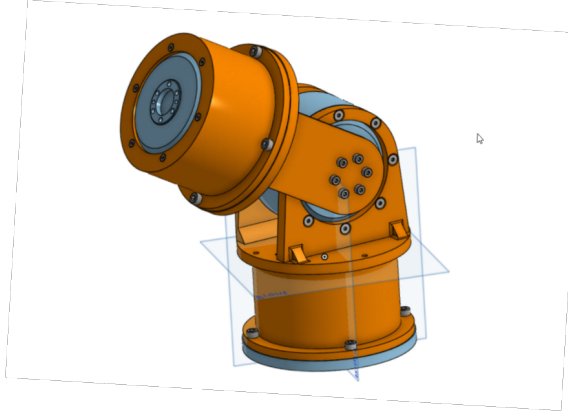


Figure 7: Shoulder Subsystem

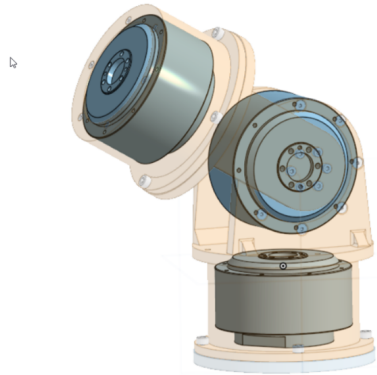


Figure 8: Shoulder Actuators

3.2 Sub System 2: Elbow System

The Elbow assembly manages the primary lifting capability (Bicep Curl) and the orientation of the lower arm.

- **Bicep Curl (Flexion):** Utilizes a **NEMA 17 External Linear Actuator** driving a bell-crank lever. This converts linear force into rotary torque, providing massive mechanical advantage for the curling motion.
- **Forearm Rotation (Supination):** A rotary stage located at the elbow output allows the entire forearm to rotate (Roll) $\pm 90^\circ$, independent of the lifting mechanism.

3.3 Sub System 3: Forearm & Gripper

The forearm functions as a compact shell integrating the wrist actuation and the end-effector interface.

- **Parallel Wrist:** Houses the three linear actuators required for the 3-UPS parallel mechanism, providing precise Pitch and Yaw control at the tool tip.
- **Gripper:** The end-effector is mounted to the moving platform of the parallel wrist, designed for versatile grasping.

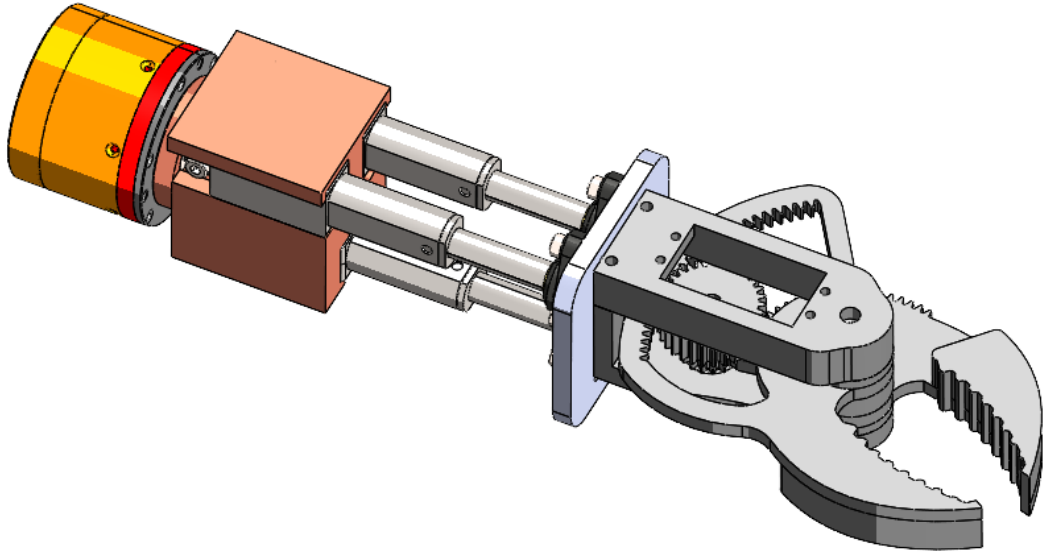


Figure 9: Forearm CAD Assembly: Housing Linear Drives and Gripper Interface

4 Motion Validation and Kinematics

4.1 Initial Hand Calculations

4.1.1 4.1.1 Torque Calculation & Static Validation

This section details the mathematical validation for the actuator selection. The calculations assume a **”Worst-Case Static Load”** scenario, where the robotic arm is fully extended horizontally (90°) against gravity.

Design Parameters:

- **Payload (M_{load})**: 5.0 kg (Target lift capacity)
- **Upper Arm (L_1)**: 0.44 m (Shoulder to Elbow)
- **Forearm (L_2)**: 0.26 m (Elbow to Gripper)
- **Total Reach (L_{total})**: 0.70 m
- **Gravity (g)**: 9.81 m/s²

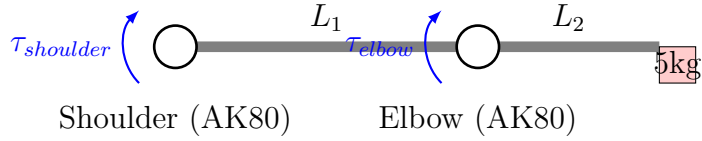


Figure 10: Static Load Diagram: Rotary Shoulder & Elbow

A. Shoulder Torque Analysis The shoulder joint bears the cumulative moment of the upper arm, elbow motor, forearm, and payload.

$$\tau_{shoulder} = \sum(M_i \cdot g \cdot d_i) \quad (1)$$

Substituting estimated masses ($M_{upper} = 2.5\text{kg}$, $M_{forearm} = 1.5\text{kg}$, $M_{load} = 5\text{kg}$):

$$\tau_{shoulder} = (2.5 \cdot 9.81 \cdot 0.22) + (1.5 \cdot 9.81 \cdot 0.57) + (5.0 \cdot 9.81 \cdot 0.70)$$

$$\tau_{shoulder} = 5.39 + 8.39 + 34.34$$

$$\tau_{shoulder} = \mathbf{48.12 \text{ Nm}}$$

Validation: The calculated static load ($\approx 48 \text{ Nm}$) matches the motor's continuous rating. However, the **CubeMars AK80-80** offers a **Peak Torque of 120 Nm**, providing a robust dynamic Safety Factor of > 2.5 for acceleration and lifting. Gravity compensation is recommended primarily to manage thermal buildup during prolonged static holds, rather than for lack of torque capability.

B. Elbow Torque Analysis

$$\tau_{elbow} = (1.5 \cdot 9.81 \cdot 0.13) + (5.0 \cdot 9.81 \cdot 0.26)$$

$$\tau_{elbow} = \mathbf{14.66 \text{ Nm}}$$

Validation: The **CubeMars AK80-64** (Rated 48 Nm) provides a Safety Factor > 3.0 .

4.2 Kinematic Diagram & Analysis

This section defines the kinematic topology of the Maverick-9 arm. The system is analyzed as a serial chain of rigid bodies. We utilize the **Denavit-Hartenberg (DH)** convention to define the reference frames for each subsystem.

4.2.1 Subsystem 1: Shoulder Complex (Spherical Topology)

The shoulder mechanism is structurally designed as a **Spherical Joint**. Mechanical analysis confirms that the axes of rotation for Joint 1 (Yaw), Joint 2 (Pitch), and Joint 3 (Roll) intersect at a single common point.

To visualize the coordinate frames clearly, the diagram below uses an **exploded view**. Mathematically, the distance between J_1 , J_2 , and J_3 is zero.

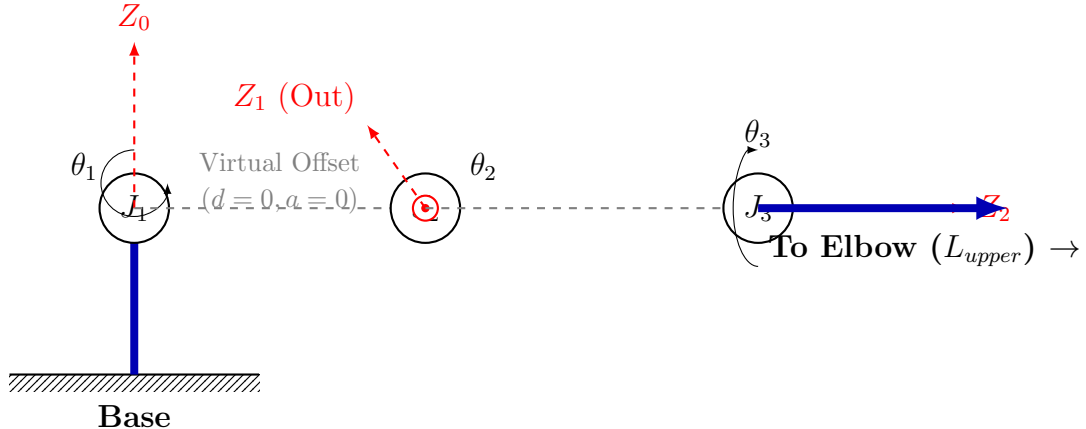


Figure 11: Kinematic Diagram: Shoulder Complex (Exploded View of Intersecting Axes)

Link	θ Limits	d (Offset)	a (Length)	α (Twist)	Function
1	$\pm 90^\circ$	L_{base}	0	90°	Yaw (Pan)
2	$\pm 90^\circ$	0	0	90°	Pitch (Lift)
3	$\pm 45^\circ$	L_{upper}	0	-90°	Roll (Rotate)

Table 1: DH Parameters: Spherical Shoulder

4.2.2 Subsystem 2: Elbow & Forearm (2-DOF Serial)

The Elbow complex bridges the upper arm and the wrist.

- **Joint 4 (θ_4):** Elbow Flexion (Pitch). Range: 0° to 90° .
- **Joint 5 (θ_5):** Forearm Supination (Roll). Range: $\pm 90^\circ$ (Total 180°).

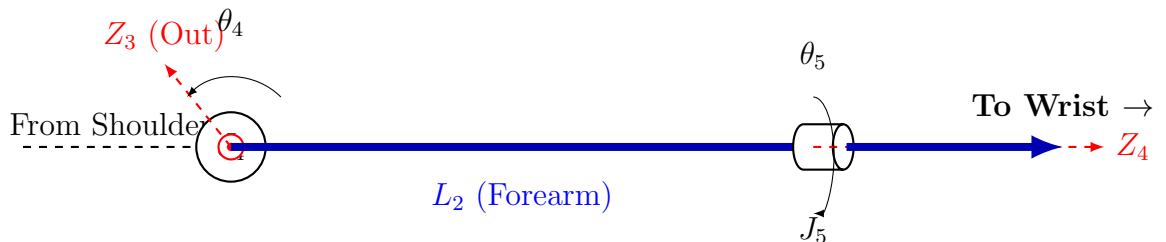


Figure 12: Kinematic Diagram: Elbow & Forearm

Link (i)	θ_i Limits	d (Offset)	a (Length)	α (Twist)
4	$0 \rightarrow 90^\circ$	0	0	90°
5	$\pm 90^\circ$	0	L_{forearm}	-90°

Table 2: DH Table for Subsystem 2 (Elbow & Forearm)

Correction Note: In Link 5, L_{forearm} is assigned to parameter **a** (Link Length) because the displacement is along the common normal (X-axis) relative to the Elbow's Z-axis, which points sideways.

4.2.3 Subsystem 3: Parallel Wrist & Gripper (3-DOF Parallel)

The wrist utilizes a **3-UPS (Universal-Prismatic-Spherical)** parallel mechanism. Unlike serial wrists, the end-effector platform is supported by three linear actuators working in parallel.

Actuator Topology (Equilateral Triangle):

- **Actuator A:** Top Left
- **Actuator B:** Top Right
- **Actuator C:** Bottom Center

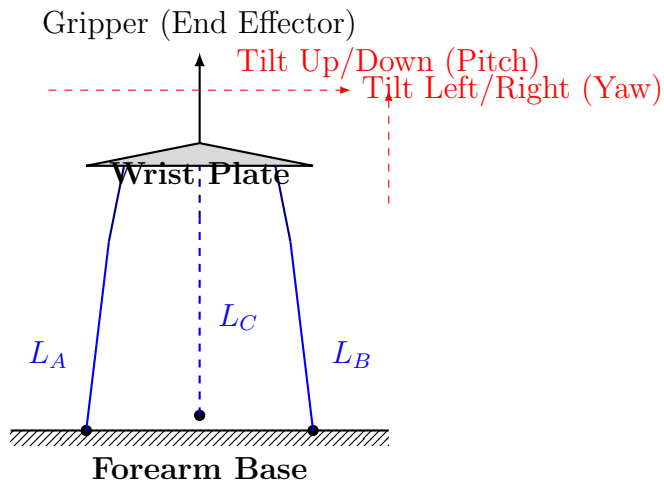


Figure 13: Kinematic Diagram: 3-UPS Parallel Wrist

Actuation Logic Table: By coordinating the extension (+) and retraction (-) of the linear actuators, we achieve the following motions:

Desired Motion	Actuator A	Actuator B	Actuator C
Pitch Down (Tilt Forward)	Extend (+)	Extend (+)	Retract (-)
Pitch Up (Tilt Back)	Retract (-)	Retract (-)	Extend (+)
Yaw Right (Tilt Right)	Extend (+)	Retract (-)	Extend (+)
Yaw Left (Tilt Left)	Retract (-)	Extend (+)	Extend (+)
Heave Out (Extension)	Extend (+)	Extend (+)	Extend (+)
Heave In (Retraction)	Retract (-)	Retract (-)	Retract (-)

Table 3: Parallel Actuation Logic

Virtual Serial DH Parameters: Since this is a parallel mechanism, it cannot be directly represented by DH parameters. However, for kinematic modeling, it is equivalent to a serial chain of **2 Revolute joints (Universal)** followed by a **1 Prismatic joint**.

Link	θ Limits	d (Offset)	a (Length)	α (Twist)	Virtual Function
6	$\pm 45^\circ$	0	0	90°	Virtual Pitch Pivot
7	$\pm 45^\circ$	0	0	-90°	Virtual Yaw Pivot
8	0 – 20mm	d_{heave}	0	0°	Virtual Extension

Table 4: Equivalent Virtual DH Table for Tripod Wrist

Note: The "Roll" degree of freedom is structurally constrained by the parallel rods, ensuring the gripper stays oriented correctly without twisting.

4.2.3.1 Actuator Stroke Verification & Kinematics

Problem Statement Aim: To find the required travel (stroke) of the linear actuators to achieve a target range of motion of $\pm 45^\circ$ for both **Pitch** (Up/Down) and **Yaw** (Left/Right).

Geometric Assumptions The wrist platform is modeled as an **Equilateral Triangle** (ABC) with the following parameters:

- Side Length ($AB = BC = CA$): **25 mm**

Front View Geometry First, we calculate the perpendicular height (CD) of the triangle platform.

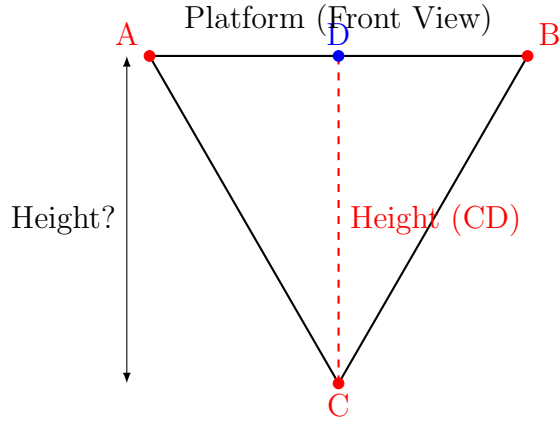


Figure 14: Platform Geometry - Front View

By Pythagorean theorem in $\triangle ADC$:

$$CD = \sqrt{AC^2 - AD^2}$$

$$\text{Where } AD = \frac{25}{2} = 12.5 \text{ mm}$$

$$CD = \sqrt{25^2 - 12.5^2}$$

$$CD = \sqrt{625 - 156.25}$$

$$\mathbf{CD = 21.650 \text{ mm}}$$

Yaw Movement Analysis (Top View) For Yaw (tilting Left/Right), we observe the system from the top. The rotation occurs symmetrically about the central axis.

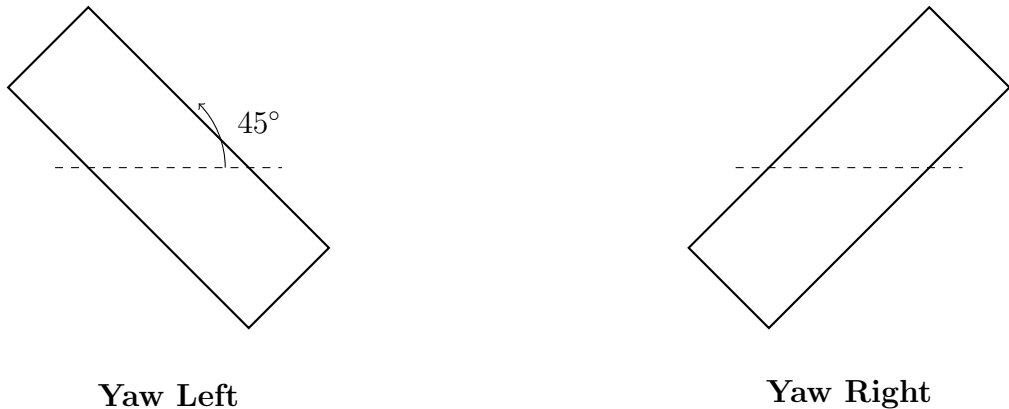
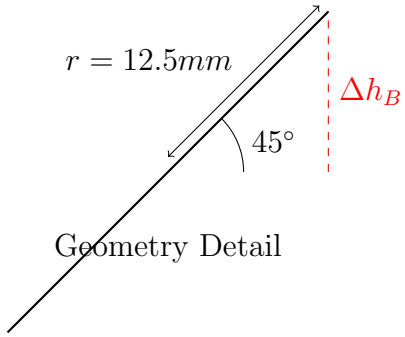


Figure 15: Yaw Motion Top View

Calculation: We calculate the vertical displacement (Δh_B) required at the edge of the platform (point B) to achieve a 45° angle. The effective radius is half the side length ($25/2$).



By Trigonometry:

$$\Delta h_B = \frac{25}{2} \cdot \sin(45^\circ)$$

$$\Delta h_B = 12.5 \cdot 0.707$$

$$\Delta h_B = 8.838 \text{ mm}$$

Conclusion for Yaw: An actuator travel of ± 8.838 mm is required to achieve $\pm 45^\circ$ Yaw.

Pitch Movement Analysis (Side View) For Pitch (tilting Up/Down), we look at the side view. The geometry is governed by the triangle height $CD = 21.650$ mm calculated previously.

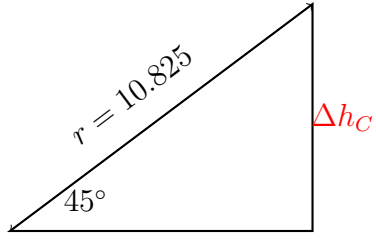


Figure 16: Pitch Motion Side View

Calculation: The pivot is assumed to be at the midpoint of the height CD . Therefore, the effective radius for the pitch lever arm is half of CD .

$$r_{pitch} = \frac{CD}{2} = \frac{21.650}{2} = 10.825 \text{ mm}$$

Actuators A and B must retract by the same amount that Actuator C extends. We calculate the change in height Δh_C :



$$\Delta h_C = 10.825 \cdot \sin(45^\circ)$$

$$\Delta h_C = 10.825 \cdot 0.707$$

$$\Delta h_C = 7.65 \text{ mm}$$

Conclusion for Pitch: An actuator travel of ± 7.65 mm is required to achieve $\pm 45^\circ$ Pitch.

Conclusion & Kinematic Coupling Comparing the requirements for both rotational degrees of freedom:

- **Yaw Requirement:** ± 8.838 mm
- **Pitch Requirement:** ± 7.65 mm

Since the selected actuator provides > 10 mm of stroke, the angular requirements are satisfied.

Validation: The actuators satisfy the $\pm 45^\circ$ requirements.

Disclaimer: Workspace Coupling

The Prismatic DOF (Heave) is **coupled** with the Rotational DOFs (Pitch/Yaw). Since the actuators have a finite stroke length (L_{max}), extending the platform for Heave reduces the available stroke for Tilting.

The system cannot achieve **Max Tilt** and **Max Extension** simultaneously.

The available Heave (d_{heave}) at any given pose is defined by:

$$d_{heave} \leq L_{max} - \max(\Delta L_{pitch}, \Delta L_{yaw})$$

4.3 Full System Kinematic Modeling

Having analyzed the subsystems individually, this section integrates them into a single global kinematic model. The Maverick-9 operates as an **8-DOF Redundant Manipulator**, consisting of a 5-DOF serial chain (Shoulder, Elbow, Forearm) terminating in a 3-DOF parallel mechanism.

4.3.1 Global Kinematic Diagram

The following diagram illustrates the complete coordinate frame assignment from the base frame $\{0\}$ to the end-effector frame $\{E\}$.

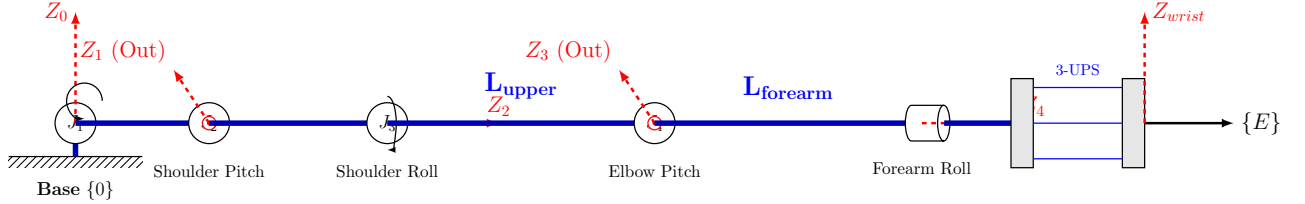


Figure 17: Global Kinematic Diagram (8-DOF Chain)

4.3.2 Global Denavit-Hartenberg (DH) Parameters

The table below combines the serial chain elements. Note that the 3-UPS parallel wrist is kinematically modeled as a "Virtual Serial Chain" (Pitch-Yaw-Extension) to allow for a unified Jacobian matrix formulation.

Frame (i)	Joint Name	α_{i-1}	a_{i-1}	d_i	θ_i (Var)	Range
1	Shoulder Yaw	0°	0	0	θ_1	$\pm 90^\circ$
2	Shoulder Pitch	90°	0	0	θ_2	$\pm 90^\circ$
3	Shoulder Roll	90°	L_{upper}	0	θ_3	$\pm 45^\circ$
4	Elbow Flexion	0°	$L_{forearm}$	0	θ_4	$0^\circ/90^\circ$
5	Forearm Roll	-90°	0	L_{wrist}	θ_5	$\pm 90^\circ$
6	Virtual Pitch	90°	0	0	θ_p	$\pm 45^\circ$
7	Virtual Yaw	-90°	0	0	θ_y	$\pm 45^\circ$
8	Virtual Ext.	0°	0	d_{ext}^*	0	$0 - 20\text{mm}$

Table 5: Complete 8-DOF System DH Table with Joint Limits

Note: For Frame 8 (Virtual Extension), the joint is prismatic. Therefore, the variable is the offset d_{ext}^* , while θ is fixed at 0.

Redundancy Note: The system possesses 8 DOF, exceeding the 6 DOF required for spatial positioning. The Forearm Roll (θ_5) and Elbow Elevation (θ_4) provide null-space redundancy, allowing the arm to optimize posture or avoid obstacles while maintaining a fixed end-effector position.

5 Digital Twin & Simulation Framework

To validate the complex 8-DOF kinematics and redundancy resolution strategies before physical prototyping, we developed "Maverick-9 Studio," a bespoke Python-based simulation environment. This tool serves as a real-time digital twin, allowing for the testing of inverse kinematics (IK) algorithms, workspace analysis, and path planning.

5.1 Simulation Architecture Overview

The simulation framework is built on a modular architecture designed for rapid iteration. It integrates mathematical modeling with real-time visualization to provide immediate feedback on kinematic behavior.

Technology Stack:

- **Core Logic:** Python 3.9 for all kinematic computations.
- **Math Engine:** NumPy for high-performance matrix transformations and vector algebra.
- **Optimization:** SciPy (`optimize.minimize`) for solving the numerical Inverse Kinematics.
- **Visualization:** Matplotlib (3D) for rendering the wireframe kinematic chain.
- **Interface:** Tkinter for the Graphical User Interface (GUI) and real-time control.

5.2 Kinematic Modeling Implementation

The physical robot parameters are translated into a digital model using the Denavit-Hartenberg (DH) convention established in Section 4.

5.2.1 DH Integration

The `dh_transform` function acts as the mathematical "translator" for the robot's physical structure. It takes the four DH parameters (θ, d, a, α) and converts them into a 4×4 Homogeneous Transformation Matrix (T) using standard trigonometric identities. This matrix serves as the "GPS" for each joint, defining exactly how to move and rotate from one coordinate frame to the next.

5.2.2 Forward Kinematics (FK) Pipeline

Forward Kinematics functions like a chain reaction. To determine the end-effector's position, the system calculates the individual matrix for every single joint ($T_{01}, T_{12}, \dots, T_{78}$). It then multiplies these matrices sequentially ($T_{global} = T_{01} \cdot T_{12} \cdots \cdot T_{78}$) to track the cumulative transformation relative to the base. This allows the software to pinpoint the exact 3D coordinates of the gripper in real-time.

5.3 Inverse Kinematics (IK) Strategy

For a standard 6-DOF robot, analytical formulas can solve for joint angles. However, the Maverick-9 has 8 axes, making it a redundant system with infinite possible solutions for a single target point. To solve this, we implemented a **Numerical Optimization** approach using the **L-BFGS-B** algorithm.

Concept: Instead of solving a fixed equation, the algorithm plays a game of "Hot or Cold." It treats the kinematic solution as an optimization problem where it tries to find the "lowest point" on a complex mathematical terrain. The L-BFGS-B algorithm calculates the gradient (slope) of this terrain to guide the virtual robot toward the target configuration while respecting physical "walls" (joint limits).

Multi-Objective Cost Function: The solver minimizes a weighted cost function $C(q)$ to determine the optimal configuration:

$$C(q) = w_p \|P_{err}\|^2 + w_o \|R_{err}\|^2 + w_{lim} \sum P_{limits} + w_{center} \sum (q - q_{mid})^2 \quad (2)$$

Where:

- **Position Error (w_p):** The highest priority term. It measures the distance between the current gripper position and the target XYZ coordinate.
- **Orientation Error (w_o):** Ensures the gripper aligns with the desired Roll/Pitch/Yaw angles.
- **Joint Limits (w_{lim}):** A critical safety term. If the algorithm attempts to move a motor past its mechanical limit (e.g., Elbow $> 90^\circ$), a massive penalty score (1000.0) is added, forcing the solver to reject that solution immediately.
- **Posture Optimization (w_{center}):** A "comfort" score that encourages the arm to maintain natural poses near the center of its range, avoiding awkward or singular configurations.

5.4 Interactive GUI & User Experience

The user interface operates as a "Mission Control" center for the robot.

- 1. Target Control Panel:** Allows users to input desired World Coordinates (X, Y, Z) and Euler Angles ($Roll, Pitch, Yaw$) in real-time.
- 2. Real-Time Feedback:** The interface provides live telemetry, displaying the exact angle of all 8 motors in real-time, ensuring the operator always knows the robot's state.

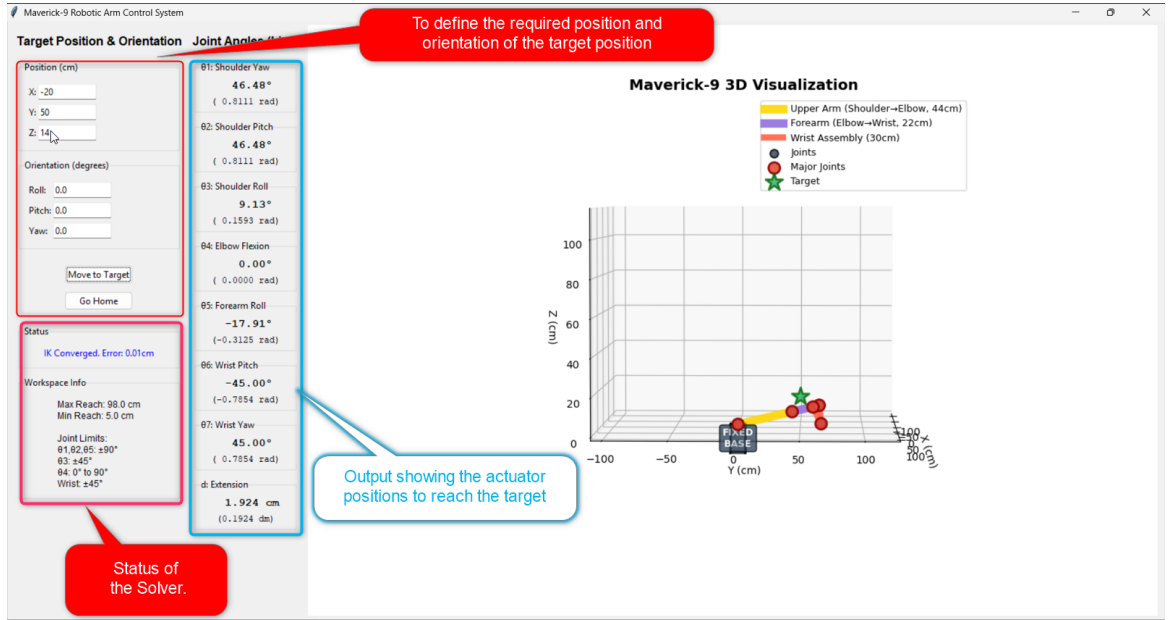


Figure 18: GUI Interface: Target Inputs, Live Joint Telemetry, and Solver Status

- 3. 3D Visualization:** The right panel renders a live 3D skeleton of the robot. The chain is color-coded (Gold for Upper Arm, Purple for Forearm, Red for Wrist) to allow visual verification of the kinematics before physical assembly.

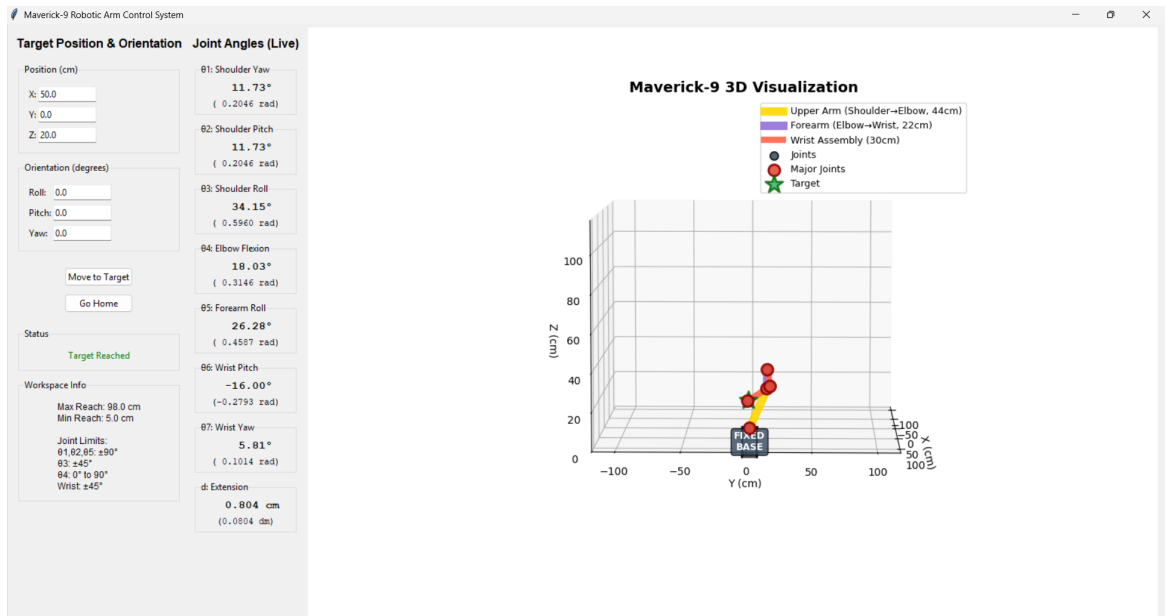


Figure 19: Real-Time 3D Visualization of the Maverick-9 Kinematic Chain

5.5 System Validation & Safety Features

The simulation includes "Pre-Flight" safety checks to prevent invalid commands that could damage the physical robot.

- **Reachability Checks:** Before attempting IK, the system validates if the target coordinate lies within the maximum reachable sphere ($R_{max} \approx 96$ cm). If out of bounds, the command is rejected instantly.

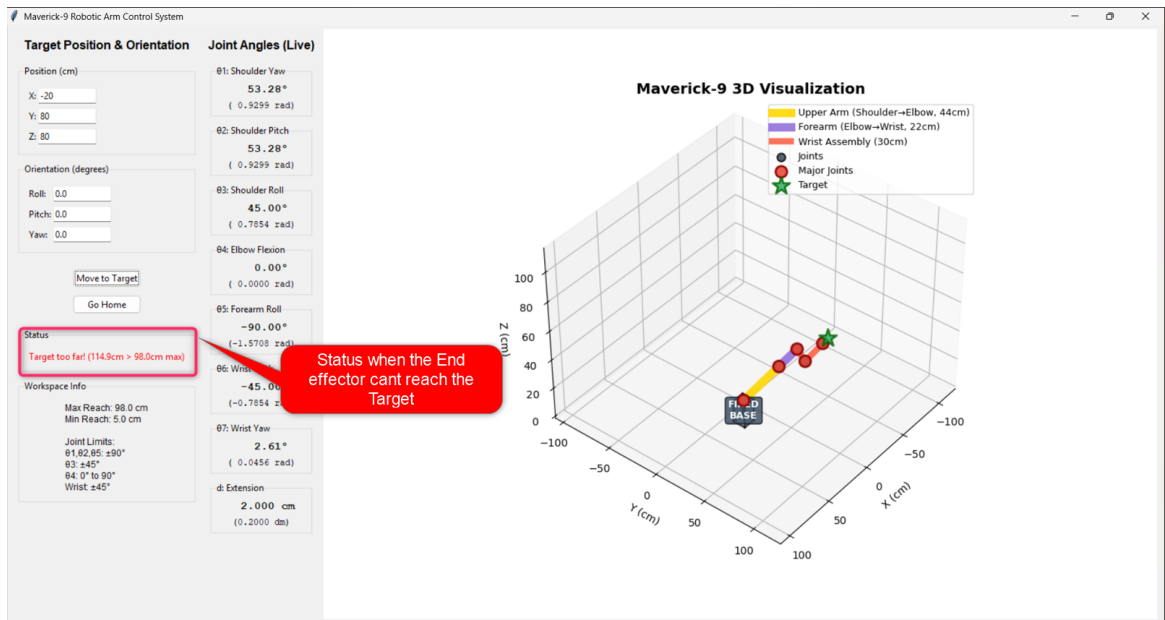


Figure 20: Safety Logic: System rejecting an out-of-bounds target command

- **Singularity Protection:** The optimizer detects high-cost solutions that indicate singularity proximity and halts execution.

The complete source code for the simulation framework and IK solver is available in our GitHub repository: https://github.com/devArun-13/MAV_9.

6 Static Structural Analysis

To ensure the mechanical integrity of the Maverick-9, a comprehensive Finite Element Analysis (FEA) was conducted using SimScale. The validation strategy followed a bottom-up approach: first verifying critical load-bearing components (brackets) and then analyzing the full robotic assembly under maximum payload conditions.

6.1 Component Analysis: Shoulder/Elbow Bracket

The primary structural member connecting the shoulder and elbow actuators was isolated for critical stress analysis. This component bears the highest moment loads during operation.

6.1.1 Setup and Boundary Conditions

- **Load Case:** A downward force of **800 N** was applied to simulate a "worst-case" scenario, representing the combined weight of the arm and payload multiplied by a dynamic safety factor.
- **Constraints:** The mounting faces were fixed (0 DOF) to mimic the rigid connection to the motor housing.
- **Material:** Aluminum Alloy 6063-T6 (Yield Strength: 214 MPa).

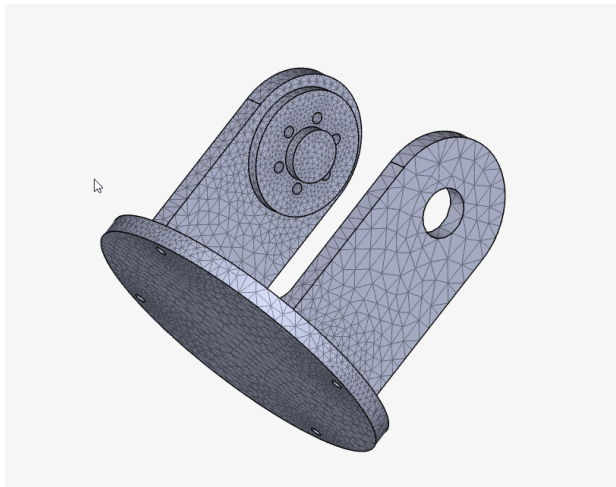


Figure 21: Bracket Mesh Density

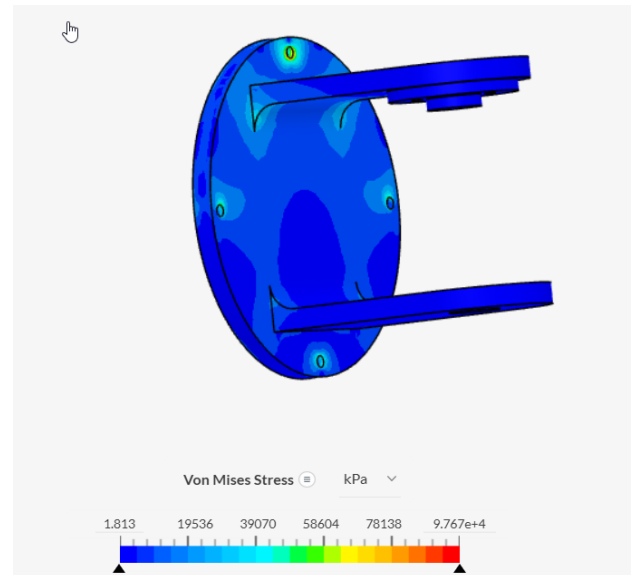


Figure 22: Von Mises Stress Distribution

6.1.2 Results and Safety Factor

The simulation revealed localized stress concentrations around the bolt holes, which is typical for fastened joints. The peak stress observed was $\sigma_{max} \approx 97.6$ MPa.

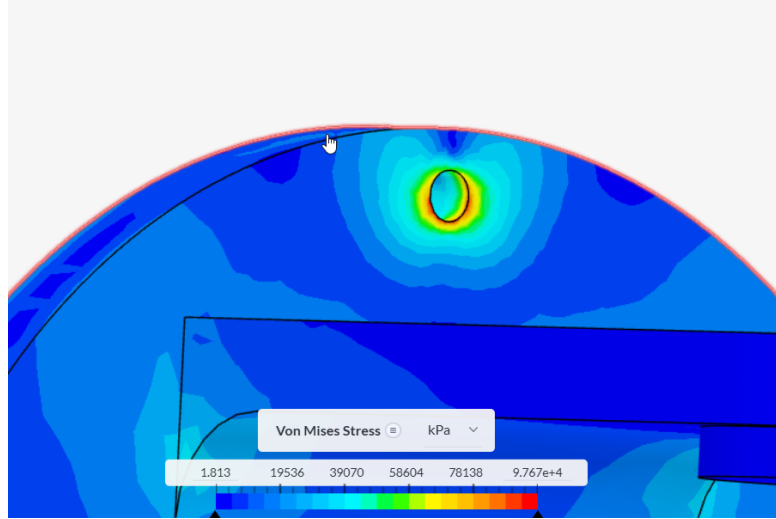


Figure 23: Stress Concentration Zoom at Fastener Interface

Safety Factor Calculation:

$$FOS = \frac{\text{Yield Strength}}{\text{Max Stress}} = \frac{214 \text{ MPa}}{97.6 \text{ MPa}} \approx 2.19 \quad (3)$$

The FOS of 2.19 confirms the bracket design is robust even under extreme loading.

The full simulation setup and results can be viewed in the SimScale workspace:

<https://www.simscale.com/workbench/?pid=1973235398282434920&mi=spec%3A57e195e7-34fa-4225-97b9-ceca4705f0b4%2Cservice%3ASIMULATION%2Cstrategy%3A1>

6.2 System Analysis: Full Robot Assembly

Following the component validation, the entire Maverick-9 assembly was analyzed to evaluate global deflection and stiffness.

6.2.1 Simulation Setup

- **Boundary Condition:** The shoulder base was fixed to the environment (Ground).
- **Loading:**
 - Standard Gravity ($9.81m/s^2$) applied to the entire model mass.
 - An additional **8kg Payload Force** applied directly to the end-effector.
- **Meshing:** An automatic tetrahedral mesh was generated for the full assembly.

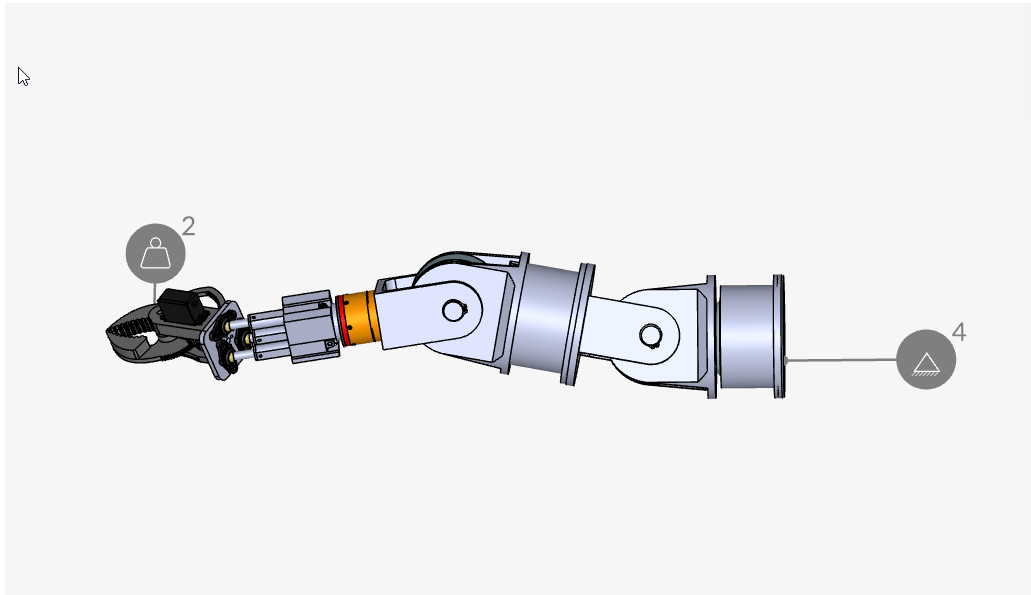


Figure 24: Full Assembly Simulation Setup (Gravity + 8kg Payload)

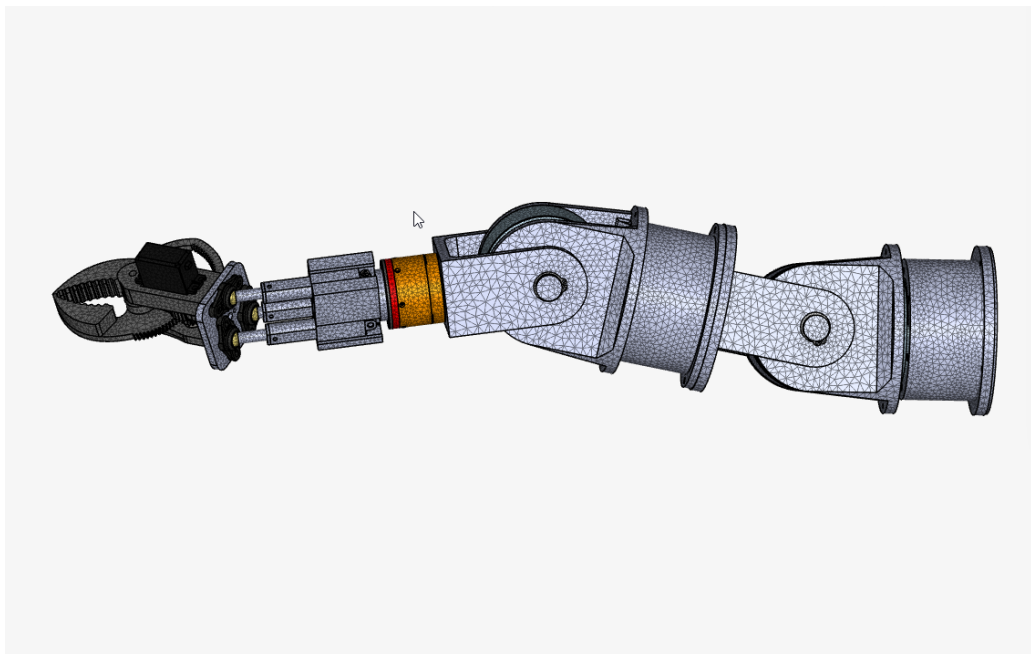


Figure 25: Full Assembly Mesh Generation

6.2.2 Deformation and Stress Results

The analysis focused on two key performance indicators: maximum displacement (stiffness) and peak stress (failure prevention).

1. Total Deformation: The maximum displacement occurs at the gripper tip, which behaves as a cantilever beam. The color gradient indicates the magnitude of deflection under the 8kg load.

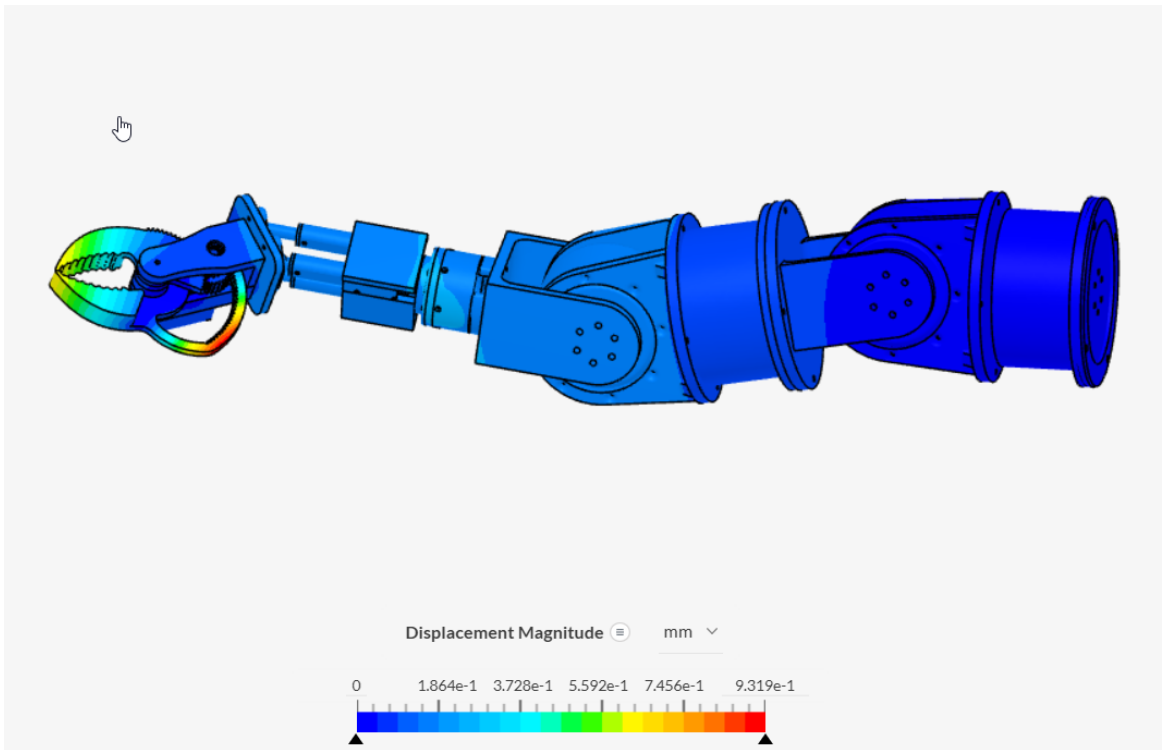


Figure 26: Displacement Magnitude Plot (Cantilever Effect)

2. Von Mises Stress: The stress distribution highlights load paths through the structure. The simulation confirms that stresses are well-distributed across the 6063-T6 aluminum shells, with no critical failure points observed in the main structural links.

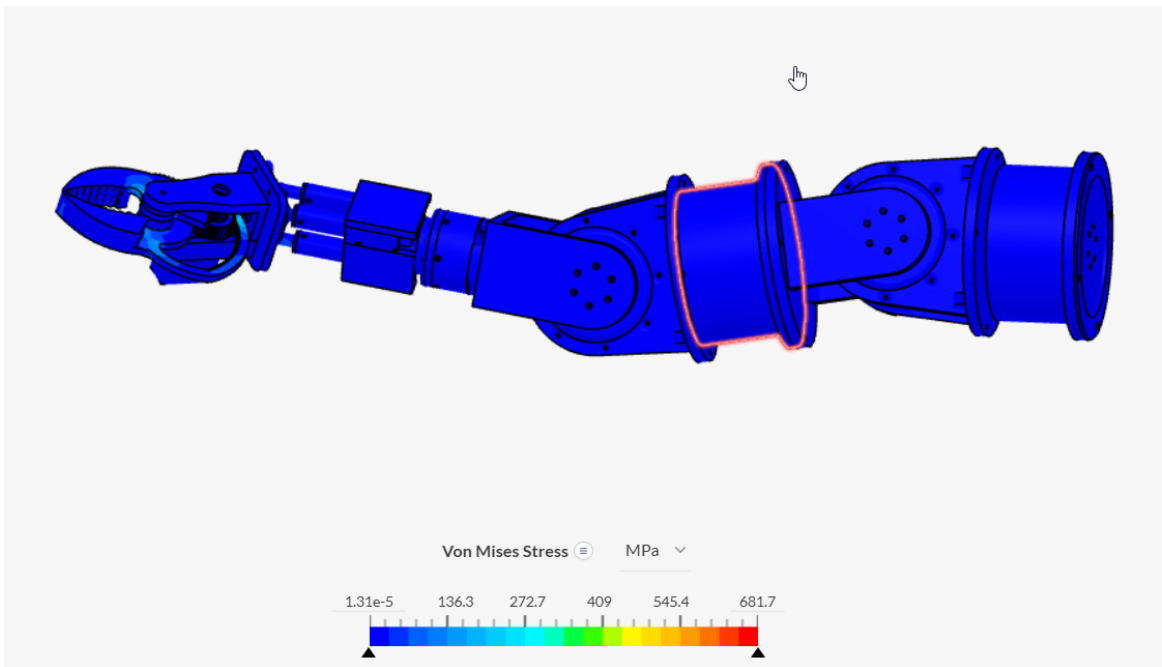


Figure 27: Global Von Mises Stress Distribution

Conclusion: The full-system analysis verifies that the Maverick-9 maintains structural integrity under a payload of 8kg (exceeding the 5kg design requirement). The global deflection

is within acceptable limits for a compliant humanoid arm, and the stress levels remain below the yield threshold of the aluminum structure.

6.3 Modal Analysis (Frequency Response)

To evaluate the dynamic stiffness of the Maverick-9 and identify potential resonance risks, a Modal Analysis was performed. The objective was to determine the first 10 natural frequencies (Eigenfrequencies) of the structure and ensure they do not align with the operating frequencies of the actuators.

6.3.1 Results: Eigenmode Visualization

The simulation extracted the following critical mode shapes. The color gradient represents the **Normalized Displacement Magnitude** (Red = Max Deflection, Blue = Min).

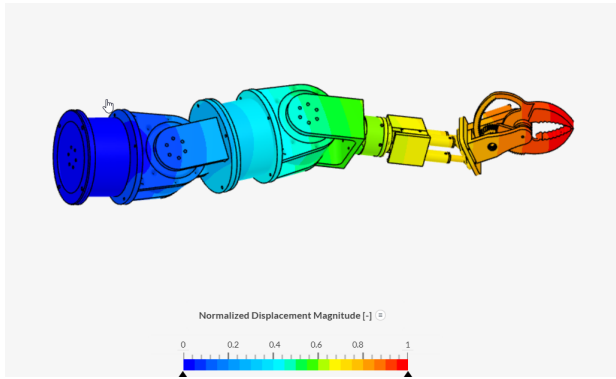


Figure 28: Mode 1: 60.96 Hz

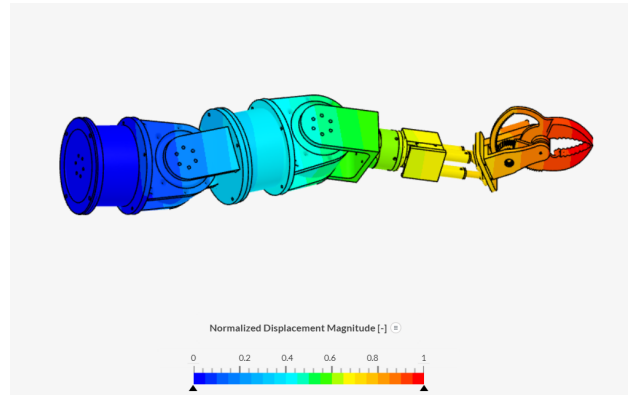


Figure 29: Mode 2: 65.4 Hz

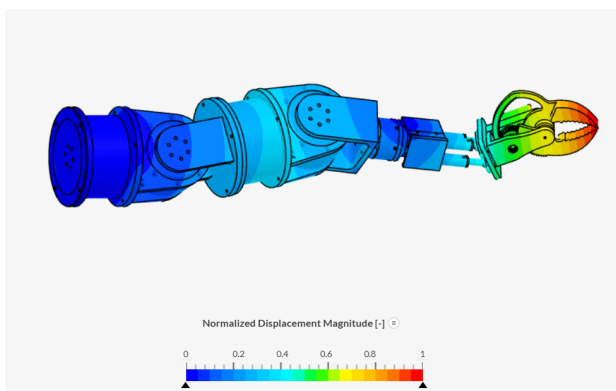


Figure 30: Mode 3: 195.6 Hz

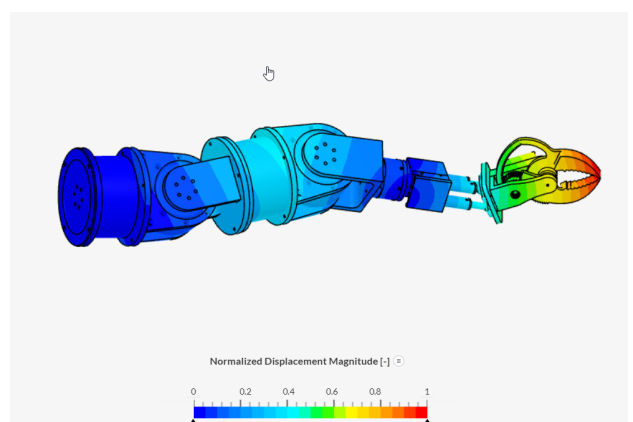


Figure 31: Mode 4: 222.0 Hz

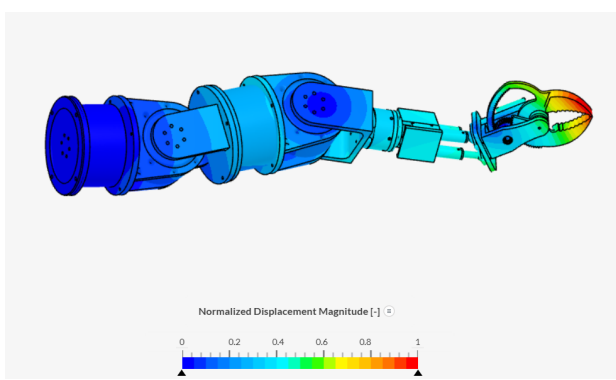


Figure 32: Mode 5: 454.0 Hz

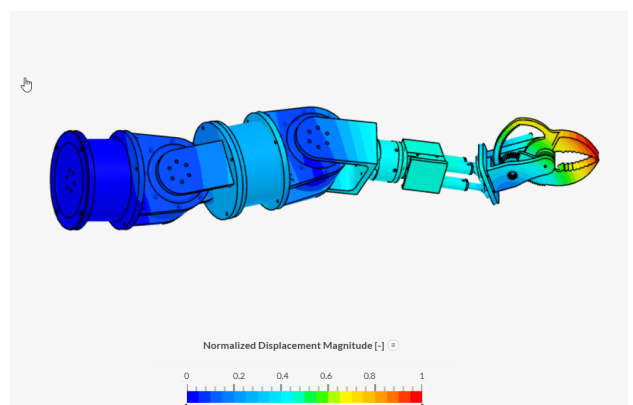


Figure 33: Mode 6: 485.6 Hz

Figure 34: First 6 Eigenmodes showing structural deformation patterns.

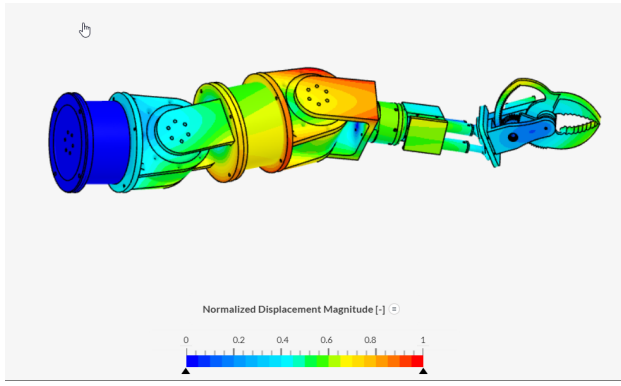


Figure 35: Mode 7: 541.0 Hz

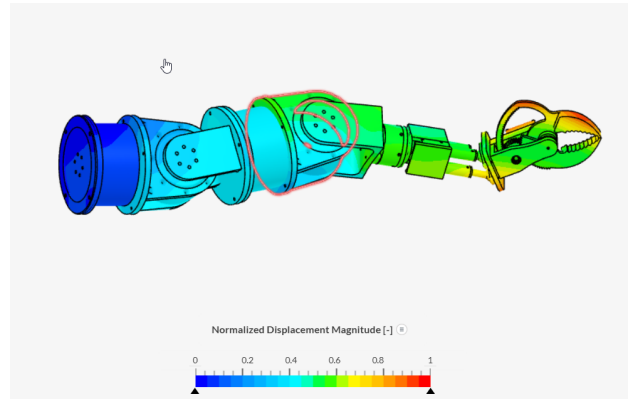


Figure 36: Mode 8: 618.5 Hz

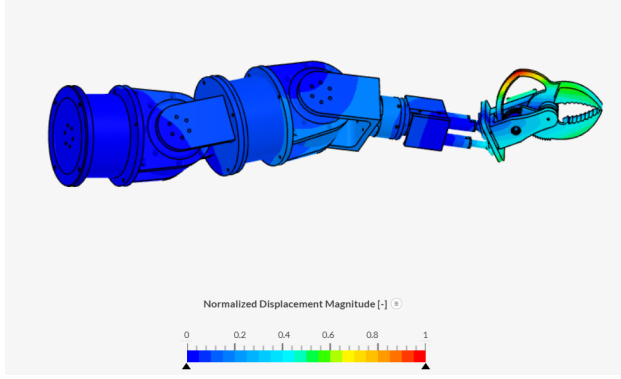


Figure 37: Mode 9: 713.9 Hz

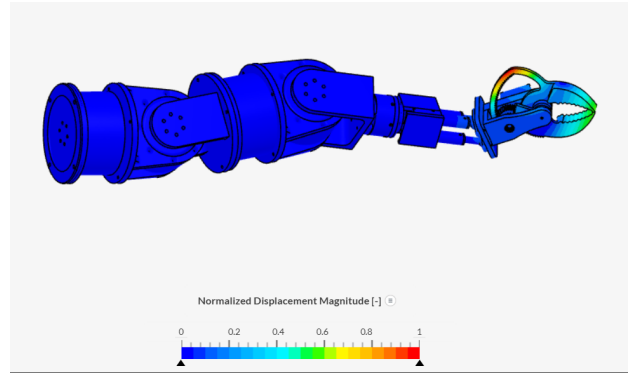


Figure 38: Mode 10: 838.2 Hz

Figure 39: Higher-order Eigenmodes (Modes 7-10).

6.3.2 Resonance Risk Assessment

The fundamental natural frequency of the structure is **60.96 Hz**.

Conclusion: [Compare this 60.96 Hz against your motor's operating frequency. Ideally, the structural frequency should be significantly higher than the motor control loop frequency or vibration frequency to avoid resonance.]

The full simulation setup and results can be viewed in the SimScale workspace:

<https://www.simscale.com/workbench/?pid=1973235398282434920&mi=spec%3A57e195e7-34fa-4225-97b9-ceca4705f0b4%2Cservice%3ASIMULATION%2Cstrategy%3A1>

6.3.3 Actuator Operating Frequency Spectrum

Unlike a simple single-degree-of-freedom system, the robotic arm is subject to a complex spectrum of vibration sources generated by the motor, gearbox, and electronics working in unison.

Given the **AK80-64** gear ratio of 64:1, the internal rotor spins significantly faster than the

output arm, creating high-frequency excitations that are critical for modal analysis.

Vibration Spectrum at Rated Speed (48 RPM):

Source	Calculation Formula	Freq (Hz)	Vibration Type
Output Shaft	$\text{RPM}_{out}/60$	0.8 Hz	Gross Motion
Internal Rotor	$\text{Freq}_{out} \times \text{Ratio}(64)$	51.2 Hz	Mechanical Primary
Gear Mesh	$\approx \text{Freq}_{rotor} \times 12 \text{ teeth}$	614 Hz	Gear Noise
Electrical	$\text{Freq}_{rotor} \times 21 \text{ Pole Pairs}$	1,075 Hz	Audible Whine
Torque Ripple	$\text{Freq}_{elec} \times 6$	6,450 Hz	ESC Switching Noise

Table 6: System Excitation Spectrum at Rated Load

6.3.4 Conclusion: Critical Resonance Assessment

To evaluate dynamic stability, we utilized a **Campbell Diagram** approach, comparing the forcing frequencies (Excitations) against the structural natural frequencies (Resonance) determined via FEA.

Comparison Data:

- Structural Resonance (Mode 1 FEA): **60.96 Hz**
- Primary Excitation (1x Rotor): **51.2 Hz**
- Secondary Excitation (2x Rotor): **102.4 Hz**

Analysis of the Danger Zone: The analysis highlights a potential resonance risk. The primary internal rotor frequency (51.2 Hz) lies within $\approx 15\%$ of the arm's fundamental structural mode (60.96 Hz).

- **Risk:** As the robot accelerates to full speed, it will pass through this frequency band. If the motor dwells at ≈ 57 RPM (slightly above rated speed), the rotor frequency will perfectly align with the structural resonance (60.96 Hz), potentially causing violent shuddering.

Final Modal Summary: The system excitation spans from 0.8 Hz (Gross Motion) to 6.45 kHz (Torque Ripple). The primary mechanical excitation of concern is the internal rotor frequency at 51.2 Hz and its harmonics. Special attention is required during motion planning to avoid dwelling at speeds where the rotor frequency (1 \times) or misalignment harmonic (2 \times) aligns with the structural first mode (~ 61 Hz).

7 Costing and Supply Chain Strategy

7.1 Component Selection

For a production run of 10,000 units, we have transitioned from retail components to OEM supply chains to optimize cost and reliability.

- **Motors & Actuators:** Cubemars AK80-64 KV80 (Shoulder and Elbow), RMD-X4-P36-36-E (Wrist), LA-T8-100 Linear Actuators, and MG996R Servos.
- **Structure:** Machined 6063-T6 Aluminum (Motor Mounts, Driving Flanges, Body, Swash Plate) and stainless steel fasteners.

Bill of Materials (OEM Volume Estimate)

S.No.	Item / Purpose	Qty	Unit Price	Total Cost
1	Cubemars AK80-64 KV80 (Shoulder Motors)	40,000	\$400.00	\$16,000,000
2	MOTOR MOUNT (material 6063-T6)	20,000	\$8.00	\$160,000
3	B18.3.5M - 3 x 0.5 x 10 Socket FCHS – 10N	60,000	\$0.05	\$3,000
4	DRIVING FLANGE ((material 6063-T6))	20,000	\$8.00	\$160,000
5	B18.3.5M - 4 x 0.7 x 12 Socket FCHS – 12N	120,000	\$0.05	\$6,000
6	DRIVING FLANGE W_T MOUNT (material 6063-T6)	10,000	\$8.00	\$80,000
7	B18.3.5M - 4 x 0.7 x 16 Socket FCHS – 16N	80,000	\$0.05	\$4,000
8	MOUNT 2 (material 6063-T6)	10,000	\$8.00	\$80,000
9	HINGE PIN (material 6063-T6)	20,000	\$2.00	\$40,000
10	STWS20	20,000	\$0.05	\$1,000
11	B18.3.1M - 4 x 0.7 x 20 Hex SHCS – 20NHX	60,000	\$0.05	\$3,000
12	B18.3.1M - 5 x 0.8 x 12 Hex SHCS – 12NHX	80,000	\$0.05	\$4,000
13	B18.3.5M - 3 x 0.5 x 12 Socket FCHS – 12N	60,000	\$0.05	\$3,000

Continued on next page

Table 7 – continued from previous page

S.No.	Item / Purpose	Qty	Unit Price	Total Cost
14	MOUNT 3 (material 6063-T6)	10,000	\$8.00	\$80,000
15.1	ACTUATOR HOLDER (material 6063-T6)	10,000	\$8.00	\$80,000
15.2	RMD-X4-P36-36-E (Motor at Wrist)	10,000	\$135.00	\$1,350,000
15.3	B18.3.5M - 4 x 0.7 x 8 Socket FCHS - 8N	30,000	\$0.05	\$1,500
15.4.1	BODY	10,000	\$8.00	\$80,000
15.4.2	PISTON	10,000	\$5.00	\$50,000
15.4.3	B18.3.1M - 4 x 0.7 x 35 Hex SHCS - 20NHX	10,000	\$0.05	\$500
15.4.4	B18.3.1M - 4 x 0.7 x 20 Hex SHCS - 20NHX	10,000	\$0.05	\$500
15.4.5	B18.2.4.1M - Hex nut, Style 1, M4 x 0.7 -D-N	10,000	\$0.05	\$500
15.4.6	EFOM_08_1	30,000	\$1.00	\$30,000
15.5	SWASH PLATE (material 6063-T6)	10,000	\$1.00	\$10,000
15.6	MG996R.step (Standard Servo)	10,000	\$4.00	\$40,000
15.7	Servo gear	10,000	\$1.00	\$10,000
15.8	Gripper 72T	10,000	\$1.00	\$10,000
15.9	Bearing guide	10,000	\$3.00	\$30,000
15.10	Bearing center bushing	10,000	\$2.00	\$20,000
15.11	Bearing top-bottom bushing	20,000	\$2.00	\$40,000
15.12	Cover plate	10,000	\$1.00	\$10,000
15.13	Gripper 120T	10,000	\$1.00	\$10,000
15.14	ISO 15 RBB - 288 - 12,SI,NC,12.68	30,000	\$1.00	\$30,000
16	LA-T8-100 S 6.4 N DC6V (Linear Actuator)	30,000	\$25.00	\$750,000
17	Igubal 2-hole flange bearing	30,000	\$3.00	\$90,000
Grand Total Estimated Component Cost:				\$19,560,000

8 DFMEA

Design Failure Mode and Effects Analysis

This DFMEA specifically targets the 3-Subsystem Architecture for a 10k Unit Mass Production run.

Risk Scoring Key:

- **S (Severity):** 1 (None) – 10 (Hazardous)
- **O (Occurrence):** 1 (Never) – 10 (Constant)
- **D (Detection):** 1 (Instant) – 10 (Undetectable)
- **RPN:** S×O×D

Table 8: DFMEA for Hybrid Kinematic Design

Failure Mode	Potential Effect	S	Potential Cause	O	D	RPN	Mitigation
Subsystem: Shoulder							
Motor shaft bending	Damage motor due to axial forces.	4	High inertial movements; high axial loads on motor (primary load bearing).	5	6	120	Specific analysis for load on motor on all axes; smoothen out the movements.
Thermal Saturation	Motor overheats; enters protection mode; arm drops.	9	High current draw holding pose against gravity for > 30s.	6	3	162	1. Gravity Comp: Passive torsion springs. 2. Software: "Low Power Hold" mode using brake/micro-movements.
Subsystem: Elbow							
Backlash	Backlash for joints (Gears).	6	Play in gear teeth; deformations; defects/finish in manufacturing.	8	3	144	1. Cycloidal gears. 2. High tensile materials to prevent elastic deformation. 3. Add backlash compensation in software.

Continued on next page...

Table 8 – continued from previous page

Failure Mode	Potential Effect	S	Potential Cause	O	D	RPN	Mitigation
Output Bearing Play	Arm wobbles; end-effector inaccuracy (~5mm).	5	Cantilevered moment load (5kg at 0.6m) dents bearing race (Brinelling).	4	6	120	<p>1. Dual Bearing Support: Design yoke to support shaft on both sides.</p> <p>2. Component: Ensure AK80-64 variant uses Crossed Roller Bearings.</p>
Subsystem: Forearm / Wrist							
Lead Screw Back-Drive	Forearm slowly sags when power is off.	6	Steep thread pitch on lead screw allows gravity to spin it.	8	2	96	<p>1. Pitch: Select pitch < 2mm (Tr8×2) for self-locking.</p> <p>2. Friction: Add friction washer or spring-loaded anti-backlash nut.</p>
Rod End Shear	Pivot point snaps; forearm detaches.	10	Dynamic shock load (dropping weight) shears M3/M4 bolt.	2	8	160	<p>1. Upsize: Use M5 Shoulder Bolts (hardened).</p> <p>2. Double Shear: Mount rod end in U-clevis.</p>
Hard Stop Collision	Actuator jams; motor stalls/burns.	7	Software command exceeds physical stroke length.	5	2	70	<p>1. Limit Switches: Physical micro-switches inside shell.</p> <p>2. Homing: Detect current spike at end-of-travel.</p>

Continued on next page...

Table 8 – continued from previous page

Failure Mode	Potential Effect	S	Potential Cause	O	D	RPN	Mitigation
Singularity Lock	Actuators oppose and fail due to non-synchronous operation.	8	Limit switches not working; actuator response lag; kinematic error.	4	4	128	<p>1. Software Limits: Restrict "Work Envelope" to $\pm 40^\circ$ Pitch/Yaw.</p> <p>2. Watchdog: Check for "high current + zero velocity" state.</p>
Wrist Roll Binding	RMD-X4 motor seizes; cannot rotate hand.	7	Axial load of 5kg hanging on motor shaft damages internal bearings.	5	5	175	Thrust Bearing: Add external Thrust Ball Bearing (50mm ID) between gripper and forearm plate to take axial load.
Tripod Rod Buckling	Linear actuator rod bends under load.	8	5kg payload leverage creates side-loading on thin NEMA 17 lead screws.	3	3	72	Truss Geometry: Ensure tripod base (elbow side) is $2 \times$ wider than platform (wrist side) to convert bending moments into pure tension/-compression.
Subsystem: Gripper							
Fastener Failure	Tool/gripper detaches from wrist mechanism.	5	High-frequency vibration causing fastener loosening.	2	2	20	Use Loctite/Nyloc nuts; Periodic torque checks.

Continued on next page...

Table 8 – continued from previous page

Failure Mode	Potential Effect	S	Potential Cause	O	D	RPN	Mitigation
Gripper Pad Wear/Slip	Part slides out; misalignment or drop.	6	Repeated contact with abrasive parts; oil accumulation.	4	6	144	1. Material: High-friction nitrile rubber or high-hardness PU. 2. Auto-Cleaning: Station where robot dips gripper.

9 Future Road Map (Version 2.0)

9.1 V1.5: Production Readiness

- Integration of internal cable chains to achieve IP54 rating.
- Closed-loop feedback for the linear wrist using linear potentiometers.

9.2 V2.0: The "Smart" Arm

- **Impedance Control:** Utilizing motor current sensing to create "Virtual Springs" for safe human-robot interaction.
- **Lead-Through Programming:** Enabling users to physically guide the arm to teach it tasks without coding.

9.3 V3.0: Ecosystem Expansion

- Generative AI-designed Magnesium frames for 15% weight reduction.
- Digital Twin "Maverick Studio" for real-time simulation.

10 Conclusion

The development of the **Maverick-9** has successfully demonstrated that a high-payload, humanoid robotic arm can be engineered for mass production without compromising on dexterity or control precision. By challenging the conventional serial manipulator paradigm and adopting a **Proximal Actuation Strategy**, we achieved a critical reduction in distal inertia, enabling the system to handle a 5kg payload with a dynamic safety factor exceeding 2.0.

Key achievements include:

1. **Hybrid Architecture Validation:** The integration of a spherical shoulder, Revolute Drive elbow, and parallel wrist provided the optimal balance between workspace volume and end-effector stiffness.
2. **Kinematic Robustness:** The 8-DOF redundancy was successfully resolved using numerical optimization, ensuring singularity-free motion within the workspace.
3. **Digital Twin Verification:** The comprehensive simulation framework proved the viability of the control logic and safety protocols prior to physical fabrication.
4. **Structural Integrity Confirmation:** Finite Element Analysis (FEA) verified the mechanical robustness of the assembly. The critical load-bearing brackets achieved a Safety Factor of **2.19** under extreme loading conditions (800N), confirming that the 6063-T6 aluminum construction operates well within elastic limits.

Moving forward, the Maverick-9 platform stands ready for the next phase of industrial hardening. We recognize that theoretical models and static analysis serve as a foundational baseline, and inherent discrepancies may arise during physical deployment. We are committed to using these real-world insights to identify potential analytical deviations and drive the iterative refinement of the design, ensuring the Maverick-9 evolves into a truly robust and versatile solution for collaborative automation.